Materials and Design 204 (2021) 109619

Contents lists available at ScienceDirect

Materials and Design

journal homepage: www.elsevier.com/locate/matdes

An open-source technology platform to increase reproducibility and enable high-throughput production of tailorable gelatin methacryloyl (GelMA) - based hydrogels

Sebastian Eggert [a,b,c,1,*], Melanie Kahl [a,d,e,1], Nathalie Bock [a,d,f,g], Christoph Meinert [a,b], Oliver Friedrich [b,e], Dietmar W. Hutmacher [a,b,d,g,h,*]

[a] Centre in Regenerative Medicine, Queensland University of Technology, Brisbane 4000, QLD, Australia
[b] School of Mechanical, Medical and Process Engineering, Science and Engineering Faculty, Queensland University of Technology, Brisbane 4000, QLD, Australia
[c] Chair of Medical Materials and Implants, Department of Mechanical Engineering and Munich School of BioEngineering, Technical University of Munich, Garching 85748, Germany
[d] School of Biomedical Sciences, Faculty of Health, Queensland University of Technology, Brisbane 4000, QLD, Australia
[e] Institute of Medical Biotechnology, Friedrich-Alexander-University Erlangen-Nürnberg, Erlangen, Germany
[f] Australian Prostate Cancer Research Centre, Institute of Health and Biomedical Innovation, Queensland University of Technology, Brisbane 4000, QLD, Australia
[g] Translational Research Institute, Queensland University of Technology, Woolloongabba 4102, QLD, Australia
[h] ARC ITTC in Additive Biomanufacturing, Queensland University of Technology, Brisbane 4000, QLD, Australia

HIGHLIGHTS

- Open-source platform overcomes manual and time-consuming processes for gelatin methacryloyl (GelMA)-based hydrogels
- High-throughput production with automated workflows yields substantial increase in reproducibility compared to manual tasks
- Materials library enables automatically production of mechanically defined 3D constructs with known parameters
- Platform offers an open-source and accessible alternative to high-priced liquid-handling robots and bioprinters

GRAPHICAL ABSTRACT

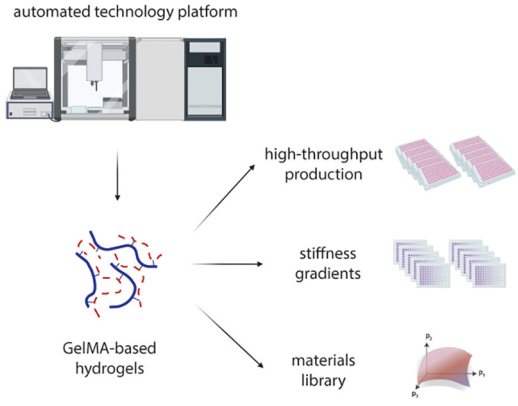

ARTICLE INFO

Article history:
Received 12 November 2020
Received in revised form 23 February 2021
Accepted 23 February 2021
Available online 27 February 2021

Keywords:
Hydrogels
3D cell culture

ABSTRACT

Gelatin methacryloyl (GelMA)-based hydrogels have become highly studied as modular tissue culture platforms due to the combination of the bioactivity of gelatin and tailorability of photo-crosslinkable hydrogels. However, current production and characterization workflows still rely on manual, time-consuming, and low-throughput processes, ultimately limiting widespread adaption. To address these challenges, an open-source technology platform is engineered and validated for automated high-throughput production of GelMA-based 3D constructs by integrating automated pipetting capabilities for viscous and non-viscous liquids. Firstly, the platform is applied in combination with inexpensive absorbance measurements to systematically optimize the mixing sequence for GelMA-based precursor solutions. This enables a decrease in the relative standard deviation of the

DOI of original article: https://doi.org/10.1016/j.ohx.2020.e00152.
* Corresponding authors at: Centre in Regenerative Medicine, Queensland University of Technology, Brisbane 4000, QLD, Australia.
E-mail addresses: sebastian.eggert@tum.de (S. Eggert), dietmar.hutmacher@qut.edu.au (D.W. Hutmacher).
[1] These authors contributed equally to this work.

https://doi.org/10.1016/j.matdes.2021.109619

Bioprinting
Tissue engineering
Gelatin methacryloyl (GelMA)
Reproducibility
Open-source

prepared mixtures from 63% to 2.5%, demonstrating a significantly improved reproducibility. Next, the applicability and high-throughput capacity are demonstrated by the reproducible generation of GelMA dilution series with 0.5 and 2% (*w*/*v*) concentration steps as well as double network hydrogels consisting of 2% (*w*/*v*) alginate and 5% (*w*/*v*) GelMA. Finally, a simple and user-friendly methodology is described that integrates Design of Experiments approaches to systematically study the combinatorial effects of material and crosslinking parameters and to establish a parameter library for on-demand production of mechanically defined GelMA-based hydrogels. The platform enables reproducible production and offers an open-source and accessible alternative to high-priced liquid-handling robots and bioprinters.

1. Introduction

Due to their inherent characteristics, such as accessibility, biocompatibility, tunability, and shape modulation ability, hydrogels are used for numerous biomedical applications [1,2]. Among those are drug delivery, soft electronics, diagnostics, and 3D cell culture [1–5]. These characteristics make hydrogels uniquely suited to provide physiologically relevant 3D microenvironments with in vivo-like biophysical and biochemical features for cell encapsulation [1,5–7]. In particular, gelatin methacryloyl (GelMA) is increasingly applied for biofabrication workflows as well as a modular tissue culture platform to study the mechanical interactions between cells and their surrounding environments. For example, Kim et al. controlled the polymerization of GelMA via differential UV penetration with a gradient photomask to demonstrate that cells plated on stiffer regions became stiffer themselves [8]. Although GelMA has been ubiquitously used for 3D cell culture in the last decade [1,2,9] and its adaption is increasing for bioprinting applications [4,10–12], current preparation and characterization workflows are still manual-based, time-consuming, and low in throughput [13]. Current laboratory automation equipment for cell culture workflows does not address the requirements for successful production of hydrogel-based 3D constructs. Essential requirements are, for example, accurate handling of viscous solutions and the different modes for crosslinking, such as photo-crosslinking. Consequently, researchers spend a substantial amount of time on repetitive and time-consuming experimental tasks. These include manual pipetting, preparation of hydrogel precursor solutions, step-by-step optimization of material and process parameters, and finally, manual production of 3D cell culture models to investigate the influence of different parameters, such as matrix stiffness, on cellular functions. These steps – mainly manual-based preparation and production – result in non-standardized handling workflows and, when added-up, contribute to significant reproducibility issues. This is of particular concern in research areas that cannot afford such irregularities. 3D cell culture models, in which hydrogels are used to investigate the influence on minute cellular functions, represents such an area, as small reproducibility issues can have critical downstream consequences on drug screening and selection.

Biomedical research has undergone increased automation and sample throughput within the last decades [14–18]. However, the preparation and characterization workflows for GelMA-based research are still mostly performed manually and hence in a low-throughput mode [13]. Although bioprinters enable the biofabrication of precise 3D constructs, only the printing process itself is automated [19–21] and hence bioprinters only enable partially automated workflows [13,21]. In addition to the low degree of workflow automation, most bioprinters only focus on the small aspect of printing and are not capable of producing a large variety of different hydrogel precursor solutions in an automated on-demand fashion. The low sample-throughput of bioprinters can, to some extent, be circumvented by adapting microarray printers, which were initially designed for DNA and protein screening and then applied to execute combinatorial screenings of microenvironmental cues on cells [22–24]. Although microarray printers automatically manufacture cell-laden 3D models to study hydrogel–cell interactions and to find optimal extracellular matrix (ECM) compositions [25], photo-induced crosslinking capabilities within an automated workflow have not been integrated yet and highly specialized equipment, such as pre-treated glass slides, are required.

To address the limitations of bioprinters and microarray printers, liquid handling robots were applied for hydrogel processing tasks due to their high degree of automation and sample throughput [26,27]. However, liquid handling robots rely on air displacement pipettes – also known as air piston pipettes – which increase the risk of air bubbles and accumulation of residues after dispensing when viscous materials, such as hydrogel stock solutions, are pipetted, leading to inaccurately dispensed volumes [28]. In addition to the particular drawbacks of each technology, most current commercial laboratory automation devices lack an open hardware and software infrastructure, preventing the integration of further customized functionalities. All of the current hardware-related solutions, which partially enable automated hydrogel processing, are tailored to a specific task and were primarily designed for either liquid or viscous handling, but not both, and furthermore, do not allow customized hardware and software modifications.

Due to the inability of automated preparation and production workflows, hydrogels are commonly characterized on a trial-and-error basis using one-factor-at-a-time (OFAT) experiments [29]. This reductionist approach neglects the interactions and dependencies of the material and process parameters and often fails to elucidate optimal factors settings. In contrast, a Design of Experiment (DoE) approach is able to identify the dependencies between various input factors and their effects on output factors [30] and provides a more detailed understanding [31,32] of the hydrogel system.

To address the current limitations, we conceptualized an open-source technology platform specifically designed to process GelMA and established a methodology to generate a material library following DoE principles. By providing automated pipetting capabilities for non-viscous and viscous solutions, the first-of-its-kind comprehensive workstation allowed automated workflows spanning from the preparation of desired hydrogel compositions, to the required mixing steps with additional bioactive molecules and/or cells, and finally, the photo-induced crosslinking of 3D constructs. A custom-written protocol design app guided the user through the parameter selection process and generated a ready-to-use protocol script that communicates with the developed Application Programming Interface (API). We report the application of the technology platform to investigate and optimize the mixing behavior for widely-used GelMA-based hydrogels to produce highly reproducible GelMA precursor solutions and manufacture GelMA-based dilution series and double network hydrogels consisting of alginate and GelMA. The integration of DoE approaches facilitated a systematic and efficient investigation of the material design factors to establish a parameter library for GelMA-based hydrogels. The combination of the open-source technology platform with DoE approaches not only promotes a fundamental understanding of material design factor interactions, but also has practical benefits by accelerating the

preparation and production workflows for GelMA-based hydrogels, resulting in substantial time and cost reduction.

2. Materials and methods

2.1. Study design

The aim of this study was to develop (i) open-source hardware components specifically designed for hydrogel systems and (ii) a user interface providing software control (iii) to enable reproducible workflows. The system was designed to simplify labor-intensive hydrogel-based experimentations by translating manual-based handling steps into automated workflows. This design offers the benefit of (a) conducting hydrogel-based experiments in a fully automated manner without the need for human intervention, (b) enabling systematic and efficient characterization of hydrogel systems, for example, to establish a parameter library of the material design factors, and (c) upscaling of a selected hydrogel system with parameters obtained from a previous optimization towards, for example, mechanobiology studies or drug screening applications.

2.2. Workstation development

2.2.1. Manufacturing and implementation

All components were designed in Solidworks (Solidworks 2018, Dassault Systèmes Americas, Waltham, MA, USA), and customized parts were manufactured from acrylic plates (ASTARIGLAS® GP, Mulford Plastics Pty Ltd., QLD, Australia) using a laser-cutting machine (ILS12.75, Universal Laser Systems, Inc., Scottsdale, AZ, USA). The workstation frame as well as the modules' frame were built from 30 × 30 mm aluminum-extrusion profiles with 8 mm slots (084107002, G.A.P. Engineering Pty Ltd., Australia). Linear stages were designed following the 'openbuilds' approach, purchased from OpenBuilds Part Store (NJ, USA) and operated with NEMA 23 stepper motors (1.8 degree per step, 2.8 Amp. per phase). An open-source pipetting robot (OT-One S Hood, OpenTrons, Inc., NY, USA) was integrated with modified hardware and software components to accommodate the operation of two positive-displacement pipettes (M100E and M1000E, Gilson Inc., WI, USA). In general, any air-driven and positive displacement pipette type can be integrated and operated with the developed setup. The light source of the crosslinker module consists of LED strips glued onto an acrylic plate (ColorBright™ Ultraviolet LED Strip Light, Flexfire LEDs, Inc., CA, USA). The well plate lid lifting function was implemented with vacuum suction cups (10.01.06.03511, Schmalz Australia Pty Ltd., VIC, Australia) and operated by a vacuum-generating ejector (10.02.01.00565, Schmalz Australia Pty Ltd.). Each temperature dock consists of two Peltier elements (TEC1–12706, AusElectronicsDirect, NSW, Australia), and a 60 × 80 mm aluminum heatsink to accommodate aluminum blocks (Ratek Instruments Pty Ltd., Australia) (dimensions: L95mm × W75 × H50mm).

A Raspberry Pi micro-controller (Raspberry Pi 3 Model B+, Raspberry Pi Foundation, Cambridge, UK) was implemented as the computational module to operate the workstation. The Raspberry Pi is a single-board computer with Wi-Fi capabilities and a Linux-based operating system. A commercial, open-source control board (Smoothieboard v1.1 microcontroller with Smoothieware software, www.smoothieware.org) provided a connection to peripherals, enabled communication between electronic components, and allowed operation of the specific functions. The Smoothieboard v1.1 (32-bi, 120 MHz, ARM-Cortex-M3 microcontroller) was interfaced with the Raspberry Pi and connected to the stepper motors, limit switches, and MOSFETs, which operate the light source of the crosslinker module and the pneumatic control valve. Modules were powered from a 360 W power supply with a 12 V/29A rating (819,368,021,202, MEAN WELL Enterprises Co., Ltd., New Taipei City, Taiwan).

2.2.2. Operation

The workstation is controlled by a Python script running on a Raspberry Pi with a Linux-based operating system. Detailed operational instructions, including hardware and software setup, are available [28,33] and additional documentation, including the protocol design app, is provided online via https://github.com/SebastianEggert/OpenWorkstation and https://github.com/SebastianEggert/ProtocolDesignApp. Briefly, the OpenWorkstation API has to be installed as a communication interface between the Python protocol and the control boards. Generated or custom-written protocol scripts (e.g. *protocol.py*) are then executed within a Python environment.

2.3. Assessment of pipetting performance

The pipetting performance of the integrated positive-displacement pipettes was assessed with gravimetric measurements to analyze the mass-to-volume ratio according to DIN EN ISO 8655 [34]. A protocol was scripted to operate a positive displacement pipette (M100E or M1000E, Gilson Inc., USA). After pre-wetting the tip, the test volume of the test fluid was aspirated and subsequently dispensed in a predefined vessel placed on an analytical balance (Sartorius AG, Gottingen, Germany). Individual weightings were recorded for each nominal test volume in an Excel spreadsheet. Distilled water (0.89 mPa·s at 25 °C) and 80% (v/v) glycerol (66.65 mPa·s at 25 °C) were used as testing fluids to assess the system with substrates of variable viscosities. Mass-to-volume ratio for 80% glycerol was calculated according to an available density model [35]. Experiments were conducted at 23.5 °C (± 1 °C).

Pipetting accuracy, also referred to as systematic error, was calculated by:

$$e_s = V - V_{test}$$

e_s systematic error (in μL)
$\overline{V}$ arithmetic mean of measured sample volumes (in μL)
V_{test} specified test volume (in μL)

$$e_s\ (\%) = 100\left(\frac{V - V_{test}}{V_{test}}\right)$$

Pipetting repeatability, also referred to as random error, was calculated by:

$$e_r = s = \sqrt{\frac{\sum_{i=1}^{n}(V_i - V)^2}{n-1}}$$

e_r random error (in μL)
s sample standard deviation
$\overline{V}$ arithmetic mean of measured sample volumes
V_i individual measured sample volumes
n number of measurements

$$e_r\ (\%) = \mathrm{CV} = 100\left(\frac{s}{V}\right)$$

CV coefficient of variation

2.4. Characterization of the wavelength and light intensity of the crosslinker module

The crosslinking performance was characterized by measuring the wavelength and the light intensity of the implemented LEDs. Light intensity is defined as the radiant flux received by a surface per unit area and was analyzed by irradiance measurement with an ILT1700 Research Radiometer (International Light Technologies, Inc., Peabody, MA, USA). The sensor surface of the radiometer was positioned under the

LED panel at well position A2 of a 6-well plate. A protocol was scripted with 20% stepwise decreasing PWM (Pulse Width Modulation) control values from 100% to 0% to measure the PWM-intensity-ratio. A spectroradiometer (StellarNet EPC200C, Tampa, FL, USA) was employed for spectral (peak wavelength) measurements conducted at 4 mW/cm^2.

2.5. GelMA synthesis

GelMA was synthesized using established protocols by Loessner et al. [36]. Briefly, porcine type A gelatin (porcine skin, Type A, Gelita, Australia) was dissolved in phosphate-buffered saline (PBS, pH 7.4; Invitrogen, Carlsbad, CA, USA) at 50 °C with agitation to reach a final concentration of 10% (*w*/*v*) gelatin. Next, 0.6 g methacrylic anhydride (MAAh) per gram of gelatin was added and vigorously stirred for 1 h. Unreacted MAAh and by-products were removed by dialysis against ultrapure water (MilliQ, Merck Millipore) using a 12-kDa molecular weight cut-off dialysis membrane. The macromer solution was then lyophilized and stored at −20 °C.

2.6. Optimization of automated mixing tasks

10% (*w*/*v*) GelMA precursor solutions were automatically prepared from 20% (*w*/*v*) GelMA stock solution and phosphate-buffered saline (PBS) stained with 0.2 mg/mL Orange G (O267–25, Fisher Scientific Co. L.L.C., PA, USA). By measuring the absorbance of Orange G, the distribution of the dye throughout the tube and therefore, the mixing efficiency was measured in a simple manner. Samples of 60 μL taken from four depths in the reaction tube (Fig. 4/a) with the master-mix were dispensed to a 96-microwell plate, and the absorbance was measured at 450 nm using a microplate reader (CLARIOstar, BMG LABTECH GmbH, Germany). After the establishment of an optimized mixing protocol, the suitability of the protocol was evaluated by preparing 5% and 15% (*w*/*v*) GelMA precursor solutions.

2.7. Generation of GelMA dilution series and double network hydrogels

GelMA dilution series were prepared by diluting a 20% (*w*/*v*) GelMA stock solution with PBS and supplemented with lithium phenyl-2,4,6-trimethylbenzoylphosphinate (LAP) (900889, Sigma-Aldrich Inc., USA) to a constant concentration of 0.15% (*w*/*v*). 2.5% and 0.5% (*w*/*v*) GelMA step dilutions were generated to final concentrations ranging from 0 to 17.5% (*w*/*v*) and 5 to 8.5% (*w*/*v*) GelMA, respectively. PBS was stained with 1.0 mg/mL Orange G to identify mixing results with absorbance measurements with a spectrophotometer as described before. Double network hydrogels were manufactured with final concentrations of 5% (*w*/*v*) GelMA, 2% alginate (4200001, DuPont Nutrition Norge AS d/b/a NovaMatrix, Norway) (*w*/*v*), 0.15% (*w*/*v*) LAP, and PBS as diluent. Similarly, PBS was stained with 1.0 mg/mL Orange G. All reagents and mixtures were kept at 37 °C using the temperature module to prevent thermal gelation.

2.8. Establishment of a parameter library for GelMA

Experimental planning and data analysis were performed with the Design of Experiments software MODDE® (Version 12.1, Umetrics, Sartorius Stedim Biotech GmbH, Germany). The Box-Behnken design is a three-level response-surface modeling (RSM) approach and was applied to obtain the factors for the following experimental parameters: GelMA concentration, light intensity, and exposure time (Table 1). All parameter design points, except for the central point, are located at the center of the edges of a hypercube, and on the surface of a sphere allowing us to estimate a full cubic model. In total, 13 different parameter combinations were executed with five replicates each (sample volume: 60 μL), resulting in 65 samples. Based on the suggested factors, the protocol design app was applied to generate the protocol scripts to operate the workstation.

Table 1
Factors for the design of experiments approach.

Name	Unit	Type	Use	Setting	Precision
GelMA	% w/v	quantitative	controlled	3.5 to 15	1
light intensity	mW/cm^2	quantitative	controlled	0.5 to 4	0.5
exposure time	s	quantitative	controlled	120 to 360	30

2.9. Mechanical analysis of manufactured hydrogels

The compressive modulus was determined by an immersed unconfined compression testing setting with an Instron 5567 microtester (Instron, Norwood, MA, USA) (Supplementary Fig. 1) [36]. PBS was added to the crosslinked hydrogels followed by 24 h incubation at 37 °C in humidified air to allow swelling of the hydrogels. The gels were removed manually from the well with a metal spatula, and a cylindrical specimen was punched out with a biopsy punch (Biopsy punch, 4 mm, Kai Europe GmbH, Solingen, Germany). The hydrogel disc was placed under a non-porous aluminum indenter in a PBS bath at 37 °C to mimic physiological conditions. The hydrogels were compressed with a strain rate of 0.01 mm/s until failure or maximum load of the load cell (5 N) was reached. The compressive modulus was calculated from the measured data as follows: First, the height *h* (mm) of each hydrogel was determined from the force-displacement curve. The height of the gel was defined as the point, at which the curve deviates significantly from the baseline. To obtain the stress-strain curve, the strain ε_1 (mm/mm) was calculated for each point as follows:

$$\varepsilon_1 = 1 - \frac{displacement}{h}$$

and the stress σ_1 (kPa) was calculated via the applied force *F* (N) divided by the cross-sectional area *a* (mm^2):

$$\sigma_1 = \frac{F_1}{a} * 1000$$

The compressive modulus E_c was obtained as the slope of the linear region of the stress-strain curve between 10% and 15% of the compressive strain. It can be calculated as the slope of a tangent between 10% and 15% of strain with the equation;

$$E_c = \frac{\sigma_{0.15} - \sigma_{0.1}}{\varepsilon_{0.15} - \varepsilon_{0.1}}$$

where $\varepsilon_{0.15}$ is a strain of 0.15 and $\sigma_{0.15}$ is the stress at this point, $\varepsilon_{0.1}$ and $\sigma_{0.1}$ accordingly.

The obtained compressive moduli values were analyzed with MODDE® and log-transformed (10Log(Y)) for the prediction plots.

2.10. Data preparation and statistical analysis

Acquired absorbance values were analyzed and plotted using GraphPad Prism 8 (GraphPad Software, CA, USA). Data were analyzed using one-way ANOVA with Tukey's honest significant difference post hoc test to identify differences in variances between groups. Data acquired from the compressive moduli testing were analyzed with MODDE® as described in section 2.8.

2.11. Data availability

The authors declare that all data supporting this study are available within the article, its supplementary information files or upon reasonable request to the corresponding authors. The software related to the system operationand application programming interface (API) is available at https://github.com/SebastianEggert/OpenWorkstation.

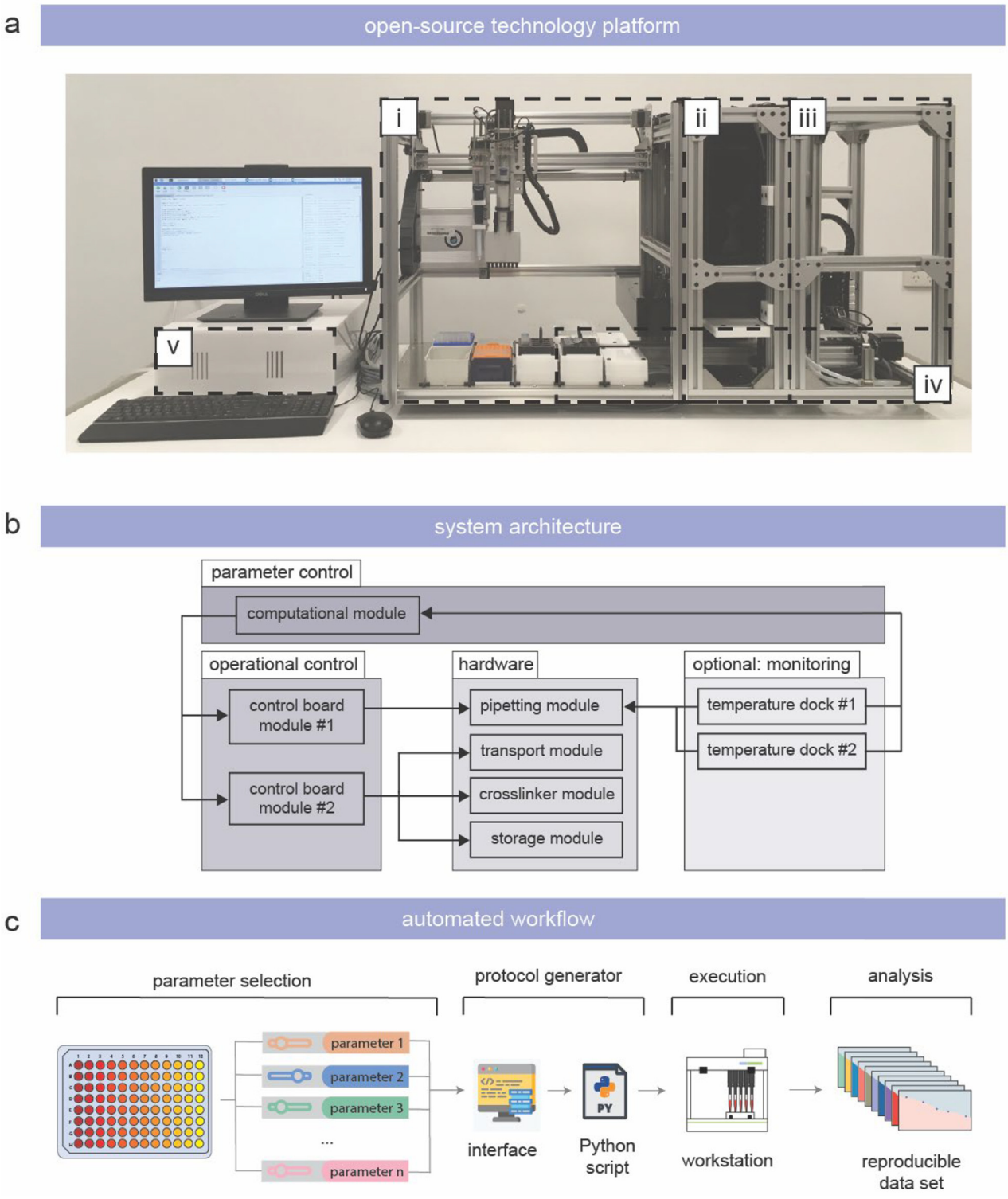

Fig. 1. Illustration of the framework for the open-source technology platform. (a) Physical setup of the technology platform, comprising (i) a pipetting/biofabrication module, (ii) a crosslinker module, (iii) a storage module, (iv) a transport module and (v) a computational module including a dedicated control box for the electrical components. (b) Introduction of the system architecture with the developed modules. (c) Display of the developed screening workflow to analyze the material design factors in an automated fashion.

3. Results and discussion

3.1. Open-source technology platform

An open-source technology platform was specifically designed to enable automated preparation and production workflows for GelMA-based hydrogels used for 3D cell culture applications (Fig. 1/a). Inspired by industrial assembly lines, a modular hardware concept was developed where the multiwell plates are transported through customizable and reconfigurable modules. The modular approach enabled versatility and flexibility, since single modules can be easily configured on demand, developed and subsequently plugged into the workstation. In addition to

the open-source technology platform concept, we targeted the integration of the following three processing capabilities for this study: pipetting capability for viscous and non-viscous materials, fully automated workflow with standardized sequences to increase reproducibility and sample throughput, and easy-to-use software supporting users to generate protocols and operate the platform. The presented workstation consists of three units linked together through a transportation system for cell culture plastics, resulting in the following four modules: pipetting module capable of handling both viscous and non-viscous liquids, well plate storage module, photo-crosslinker module, and a transportation module (Fig. 1/b). The aluminum frame provides a compact design for machine stability and portability.

The presented workstation addresses one main limitation of commercial laboratory equipment: Customization and open-source character. Commercial laboratory equipment is proprietary and cannot be modified for customized applications unless money is spent on costly upgrades. For this reason, current laboratory equipment is mostly not able to keep up with the rapid developments, in particular the emerging biofabrication requirements, in research laboratories. The presented concept provides an open-source solution, which allows not only access to hardware and software to implement customized modifications, but also a modular setup that allows the future integration of newly developed modules to increase the application range. Building upon an open-source approach, this solution provides an accessible technology platform to all researchers around the world. By doing so, the presented platform can be easily re-built by other research labs and upgraded to accommodate additional features, such as imaging modules [37,38], photometer modules [39,40] or sensor modules [41], to increase the application range. The impact of open-source laboratory automation devices is well demonstrated with the OT-2 (Opentrons, Inc., USA), which is increasingly used as an affordable and automated COVID-19 testing platform. Next to the open-source character, specific functionalities have been integrated for the automated processing of viscous solutions. It has to be noted that, for example, the FLEX workstations by Chemspeed Technologies AG (Switzerland) [42,43] and the pipetting solutions by SPT Labtech Ltd. (UK) [44] are also able to accurately pipette viscous solutions and hence hydrogel precursor solutions. While such solutions are used for pipetting tasks, they do not provide a holistic concept required for hydrogel solutions used for cell culture applications. Solutions by Chemspeed Technologies AG are mainly used for chemical tasks, such as automated peptide synthesis of peptide & oligosaccharide libraries, and customized hardware modifications would be very costly. Solutions by SPT Labtech Ltd. provide positive displacement pipettes to pipette viscous materials, but already lack temperature modules to process thermoresponsive materials and heat media to 37 degrees. Taken together, while automated solutions are partially available, they do not provide a holistic approach (Fig. 1/c) and do not allow customized hardware and software modifications by the end-user. For this reason, current laboratory equipment is mostly not able to keep up with the rapid developments and hence complex biofabrication requirements in research laboratories. The presented concept not only provides an innovative solution to automate the production of GelMA-based hydrogels, but also enables researchers to apply a do-it-yourself approach (Supplementary Video 1) to develop their own technology [45].

3.1.1. Pipetting/biofabrication module

The pipetting module was designed and developed to employ a commercial open-source pipetting robot that enables automated liquid aspiration, dispensing, and mixing tasks using standard laboratory pipettes. The capabilities of the implemented open-source pipetting robot were expanded by the integration of positive-displacement pipettes utilizing piston-driven liquid displacement for reliable pipetting of viscous and non-viscous materials (Supplementary Video 2). In addition, temperature docks were developed to control the temperature of reagents. The pipetting module can be equipped with two user-defined pipettes (single- or 8-channel pipette of any nominal volume) and up to eight containers (e.g. multiwell plates, tip racks, media and reagent reservoirs, etc.) can be positioned on the deck of the pipetting module to allow processing of any container type designed according to the ANSI/SLAS standards (ANSI: American National Standards Institute, SLAS: Society for Laboratory Automation and Screening) (Fig. 2a). In-house developed temperature docks were employed to control the temperature of the reagents between 5.5 °C and 95 °C. Since viscous materials tend to stick to the pipette tip, a simple and inexpensive tip touch function was integrated to remove excess material from the tip before dispensing (Fig. 2c). Especially the integrated temperature dock and tip touch increase the applicability for hydrogel-related applications, since customized solutions can be designed, evaluated and integrated to ensure suitable automated solutions [28]. For example, the temperature docks allow the processing of thermoresponsive hydrogels such as GelMA, matrigel, collagen, Pluronic F127 or Gellan Gum. Current bioprinters oversee post-production steps such as not accommodating for liquid handling capabilities, which are essential for media exchange for cell-laden constructs. Media, diluent or washing buffer can be prewarmed to 37 °C and dispensed into the multiwell cell culture plate without any hardware modifications. While stock solutions and precursor solutions can be easily handled with the developed system, the system is not able to handle solid materials (e.g., powders).

3.1.2. Photo-crosslinker module

Chemical crosslinking capability can be realized to enable photo-induced gelation of hydrogels supplemented with a photoinitiator system [4,7]. This capability was added to the workstation by the integration of a crosslinker module, which consists of an enclosure and one LED panel (Supplementary Fig. 2a). By engineering a plug-and-play system for the LED panel, the panel can be easily exchanged to allow the integration of LEDs with a different wavelength and, thereby, increase the range of photoinitiator systems, which can be studied with the system. By adjusting the distance of the light source to the culture plate and the supplied voltage intensity using PWM (Pulse Width Modulation) control, the protocol script regulates the applied light intensity. In the presented setup, LEDs with a wavelength of 400 nm were installed and calibrated to a light intensity of up to 4 mW/cm^2. Photo-induced crosslinking provides the ability to easily control the matrix stiffness by changing the crosslinking duration. Commercial bioprinters usually crosslink single samples and lack a function to create exposure gradients with defined durations. The crosslinker module was specifically designed to overcome this limitation by using a sliding mask to create such exposure gradients (Supplementary Fig. 2b). By moving the sliding mask to a predefined direction above the well plate, hydrogels with varied matrix stiffness are manufactured in a fully automated, controlled and highly reproducible manner. The automated control of the light intensity and the exposure duration enables a simple and automated generation of stiffness gradients in one well-plate to study mechanical cues on cellular functions [8].TT The sliding mask presents a key feature of the photo-crosslinker module and can be used to control the extent of light-mediated reactions [46]. Building upon the open-source approach, LED panels with different wavelengths can be easily designed to enable the study of additional photoinitiator systems, such as Irgacure 2959 [47], which is typically excited at 365 nm.

3.1.3. Storage module

A storage module was added to increase the overall sample throughput for the workstation. To do so, a rack with up to six multiwell cell culture plates can be equipped within the storage module to process additional samples or to archive samples for a defined time for a specific assay protocol. A custom-designed plate mover grips the well plate within the rack and positions the plate onto the transportation module. This allowed a fully automated workflow with the integrated lid lifter function using vacuum suction cups.

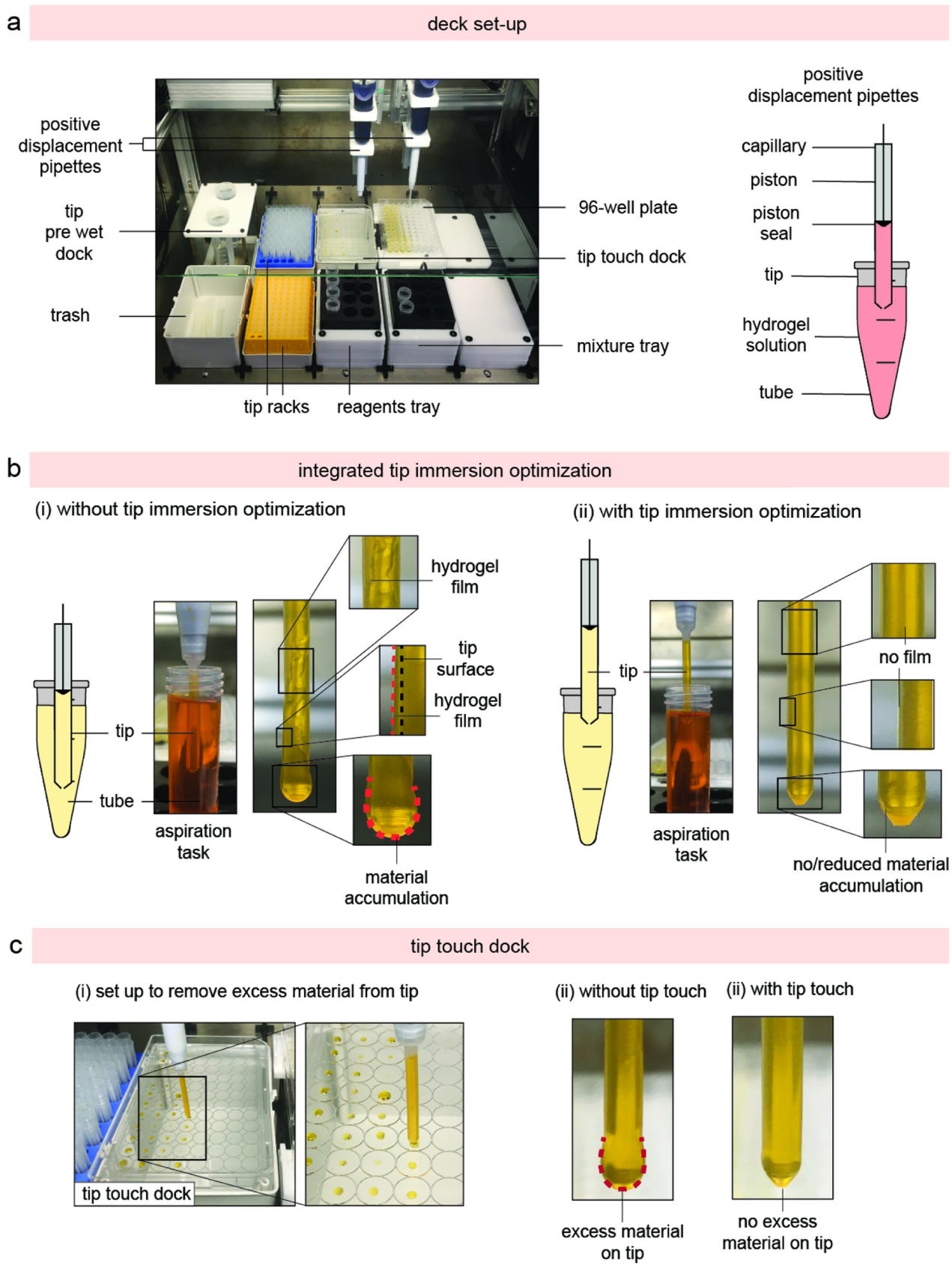

Fig. 2. Summary of the flexibility and functionalities of the workstation. (a) The pipetting/biofabrication module has an 8-deck capacity for containers designed according to the ANSI/SLAS standards. In-house developed temperature docks keep the reagents at a constant temperature during the experiment. (b) Integrated tip immersion optimization automatically calculates and applies optimal immersion depth into the hydrogel solution to reduce accumulation of material on the tip. (c) Optionally, a tip touch is integrated to remove excess material on the tip, ensuring reproducible pipetting tasks. ANSI: American National Standards Institute, SLAS: Society for Laboratory Automation and Screening.

3.1.4. Protocol design app

A graphical user interface (GUI) was programmed to remove the need to write protocol scripts by providing an intuitive interface that guides the user through the parameter selection process, generates the ready-to-use protocol code and operates the platform. The GUI is hereby referred to as Protocol Design App. In contrast to commercial interface solutions for laboratory equipment, the developed protocol design app was specifically designed for the production of photo-crosslinkabled hydrogel-based 3D constructs by presenting an intuitive workflow to select the material and process parameters (Supplementary Fig. 5). In addition, the backend automatically calculates the optimal immersion depth of the tip to avoid an accumulation of viscous material on the tip (Fig. 2b).

3.2. Characterization of the pipetting precision and accuracy

Pipetting precision and accuracy were assessed in accordance with ISO 8655, which defines the requirements to produce reliable and accurate calibration data for a piston-operated volumetric apparatus [34]. Following Bessemans et al., precision is defined as the exactness of volume displacement by the pipette and accuracy is defined as the difference between the actual transferred volume and the target volume [48]. Pipetting precision and accuracy were assessed following calibration by gravimetric analysis for positive-displacement pipettes (M100E: 10–100 µL, M1000E: 100–1000 µL) with distilled water and 80% (v/v) glycerol at room temperature (23.5 ± 1 °C) and results are displayed in Fig. 3. The assessment of the pipetting performance demonstrated permissible systematic errors (accuracy) (in µL) within acceptance criteria as specified in ISO 8655 and permissible random errors (precision) (in µL) with minor deviations from the acceptance criteria for volumes of 10 µL and glycerol pipetting tasks.

Based on the precision of automated aspirating and dispensing tasks, the developed pipetting module is expected to outperform manual pipetting accuracy, as human pipetting operators demonstrated significant intra- and inter-individual imprecision in a previous study [49]. Another important characteristic to ensure accurate and reliable pipetting is pre-wetting of the tip. Pre-wetting increases the humidity within the tip to reduce the amount of sample evaporation. Since pre-wetting leads to a significant improvement in the pipetting reliability [50], the conducted experiments were performed with tip pre-wetting with the nominal volume.

The immersion depth of the tip was identified as a critical parameter for reproducible pipetting. Especially when viscous materials were pipetted, residues of the material adhered to the outer tip surface [28] (Fig. 2b) and resulted in inaccurate pipetting. To overcome this issue, the protocol design app automatically calculated the optimal immersion depth with respect to the reaction tube, tip length, and tube volume, and added the depth to the generated protocol script. Optimized immersion depths ensure that the tip aspirates and dispenses approx. 2 to 5 mm under the material surface to avoid an accumulation of viscous materials on the tip. The calibration of the pipette plunger position (maximal and minimal volume) was identified as an additional critical parameter. As the lead screw is directly connected to the pipette's piston, the pipetting performance depended on the traveled millimeters by the lead screw-based positioning system. The initial top (maximal volume) and bottom position (minimal volume) have to be adjusted manually and saved in the calibration terminal. Hence, inaccurate calibration positions are likely to result in inaccurate pipetting performance. To prevent this, the presented validation protocol was executed after each manual calibration to assess the pipetting performance.

3.3. Characterization of the crosslinker module

Photo-induced polymerization of hydrogel precursor solutions provides an extensive tool to tailor the physical characteristics of the resulting hydrogel [47,51]. Although the crosslinking parameters are

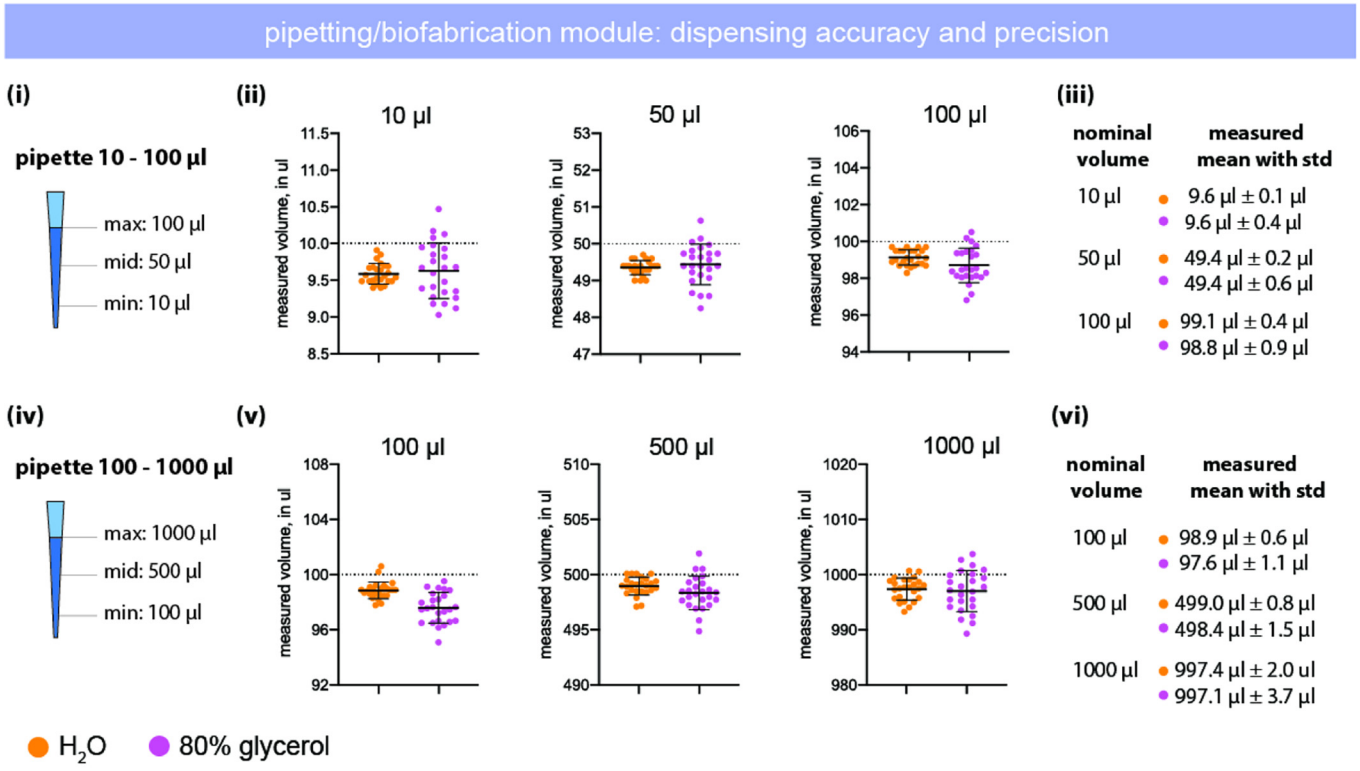

Fig. 3. Characterization of the pipetting and crosslinker performance. Pipetting accuracy and precision were evaluated for (i) a 100 µL and (iv) a 1000 µL positive displacement pipette with distilled water (orange) and 80% glycerol (pink). For each pipette, the minimum, median and maximum volume were tested and single data points are shown as measured volume in µL in graphs (means ± standard deviations, $n = 25$).

critical to generate physiologically relevant and reproducible 3D models, essential information to reproduce the results are rarely reported [52,53] or the crosslinking system is not well characterized. To provide a photo-induced crosslinking system for reproducible hydrogel polymerization, a detailed characterization of the crosslinking module was conducted. Spectral wavelength measurements yielded a symmetrical spectrum with a peak wavelength (λ_{peak}) of 407 nm (Supplementary Fig. 3a/i) and the spectrum showed 90% of the spectral power distribution between 389 nm to 432 nm (Supplementary Fig. 3a/ii). This enables photo-induced polymerization with photoinitiator systems excited in the visible light range, such as LAP [47]. Next, light intensity, defined as the radiant flux received by a surface per unit area, was measured in mW/cm^2 for different PWM values (Supplementary Fig. 3b). Changes in PWM values were used to control the supplied voltage to the LEDs and, thereby, presented a dimmer function for the light. With 100% PWM, a light intensity of 4.0 mW/cm^2 was measured inside the assembled closure at the sample position. By decreasing the supplied voltage, decreased intensity values were recorded and plotted linearly with an R-squared value of 0.9994. Compared to most crosslinking devices, this dimming function allowed the automated study of different intensities without any hardware modification by simply addressing the chosen intensity value in the protocol script.

3.4. Optimization of automated mixing tasks

Hydrogel precursor solutions are commonly prepared by mixing the required substances, including stock solutions of hydrogel prepolymers, diluents, and the photoinitiator system. Initial trials of producing hydrogel-based 3D constructs resulted in substantial variability of the compressive moduli caused by incomplete mixing between the viscous hydrogel stock solution and the diluent. Therefore, detailed characterization and optimization studies of the mixing steps between the hydrogel stock solution and the diluent were conducted. These studies resulted in mixing protocols that achieved homogenously mixed hydrogel precursor solutions and thus, reproducible hydrogels. To increase the reproducibility and minimize the standard deviation, the generation of a 10% (*w*/*v*) GelMA precursor solutions was initially optimized, and finally, the optimized mixing tasks were repeated with 5% (*w*/*v*) and 15% (*w*/*v*) GelMA. GelMA was selected for these mixing optimization tasks, as it is a widely used hydrogel for cell encapsulation studies [36,54]. To verify the homogenous mixing of the hydrogel stock solution and the diluent, the diluent was stained with Orange G and samples were taken from different immersion depths (every 2 mm) throughout the prepared hydrogel precursor solution (Fig. 4a). These samples were analyzed with a spectrophotometer to identify differences in absorbance values caused by inhomogeneous mixing [28].

3.4.1. Mixing optimization procedures to prepare 10% (w/v) GelMA

In the beginning, mixing commands were applied which consisted of a single aspiration step immediately followed by a dispensing step at a fixed position. This was repeated four times per reaction tube. This aspirating/dispensing sequence is hereby referred to as 'without *optimized mixing*'. Using this mixing sequence, absorbance measurements yielded increased values in the upper parts and lower absorbance values in the lower parts of the prepared GelMA mixture (Fig. 4b). Due to the absorbance difference, it was concluded that more PBS containing Orange G was in the upper part while more GelMA was in the lower part of the reaction tube, and the two components did not mix sufficiently. The inhomogeneous distribution was confirmed with high coefficients of variation (CV) values ranging from 10.6 to 63.1%. As more PBS was found in the upper part, the initial mixing protocol was modified with an additional step, which aspirated volume from the upper layer and dispensed it further down followed by two subsequent mixing steps (aspirating/dispensing) at this lower position. Moreover, additional movements of the pipette during the aspirating/dispensing sequence were added to optimize the mixing of viscous materials. While aspirating, the pipette moves with the falling liquid level down and then moves up again while dispensing the liquid from the pipette. This approach is also known as inverse pipetting. For further reference, this mixing action is hereby referred to as '*optimized mixing*' and was implemented as a new command into the Python script and is available in the public repository. To increase the mixing force and, thereby, also shorten the mixing time, the aspirating and dispensing speed was finally increased for all mixing tasks. These custom changes resulted in homogenous absorbance values and decreased CV values ranging from 1.4 to 2.7% (Fig. 4c).

The final optimized mixing workflow is depicted in the Supplementary Fig. 4 and consisted of (i) inverse pipetting tasks, which are operated ten times, (ii) aspiration of a defined volume in the upper layer and dispensing it into the lowest region (iii) with two conventional mixing tasks at three defined locations throughout the reaction tube, (iv) repetition of step (ii) with two conventional mixing tasks at the lowest locations, and finally (v) again inverse pipetting tasks for ten times. Since the tip immersion depth and the pipetted volumes depend both on the total volume, the reaction tube geometry and the tip length, these two parameters (depth, volume) are automatically calculated using the programmed protocol design app.

The optimization tasks and results were described in detail to provide researchers with valuable information about the influences of different mixing approaches. Although it is common knowledge that the preparation of hydrogel solutions requires sufficient mixing tasks without introducing air bubbles, we could not find a detailed study on the characterization of the mixing results and the influences of different mixing approaches. We acknowledge that not all pipetting tasks can be documented and included in a publication; however, due to these results, we hope to stimulate greater awareness for reliable and well-characterized mixing tasks. The presented setup with Orange G presents a simple, inexpensive and straightforward method to identify homogenous mixing as well as to support and verify optimization tasks.

3.4.2. Application of optimized mixing protocol to manufacture 5 and 15% (w/v) GelMA

To verify if the optimized mixing protocol not only reproducibly prepares a 10% (*w*/*v*) GelMA precursor solution but is also applicable to lower and higher concentrations, the same optimized mixing protocol was employed for the preparation of 5% (*w*/*v*) and 15% (*w*/*v*) GelMA precursor solutions (Fig. 4d). For both concentrations, four independent replicates were prepared by mixing the GelMA stock solution with the diluent and analyzing the sample positions. Thereby, not only the mixing protocol, but also the reproducibility between the independent replicates were verified. Results for 5% (*w*/*v*) and 15% (*w*/*v*) GelMA yielded CV values between 1.8 and 2.8% and 2.3 to 5.3%, respectively. These results demonstrate the applicability of the optimized mixing protocol for higher and lower GelMA concentrations, and highlight the highly reproducible mixing for a range of GelMA concentrations.

3.5. Fully automated preparation and generation of GelMA dilution series

After the establishment of an optimized mixing procedure for the generation of GelMA-based precursor solutions, the protocol design app was applied to generate protocol scripts for the generation of GelMA serial dilutions. First, a GelMA dilution series with a step size of 2.5% (*w*/*v*) ranging from 0 to 17.5% (*w*/*v*) was automatically prepared and pipetted into a 96 well plate (n = 12 per concentration) (Fig. 5a/i). PBS was stained with Orange G to verify the GelMA dilution steps and the reproducibility for each dilution with absorbance measurements. The analyzed data showed stepwise increasing absorbance values with increasing GelMA concentration (Fig. 5a/ii). Since PBS, as the diluent, was supplemented with the dye Orange G, increasing PBS volume is mixed with decreasing GelMA concentration, resulting in higher absorbance values. Statistical analysis exhibited a highly significant difference ($p < 0.0001$) between each of the 2.5% (*w*/*v*) steps. Linear regression

a

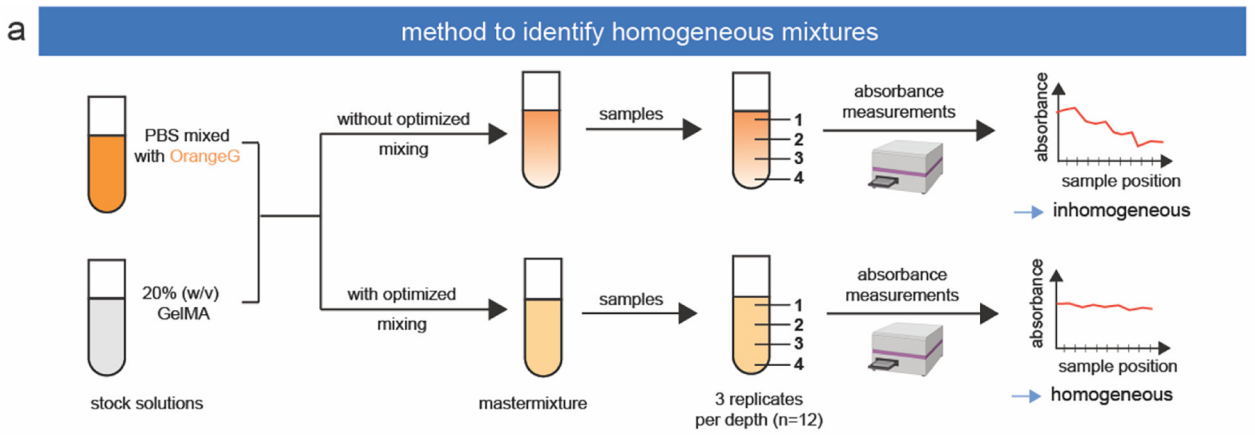

b

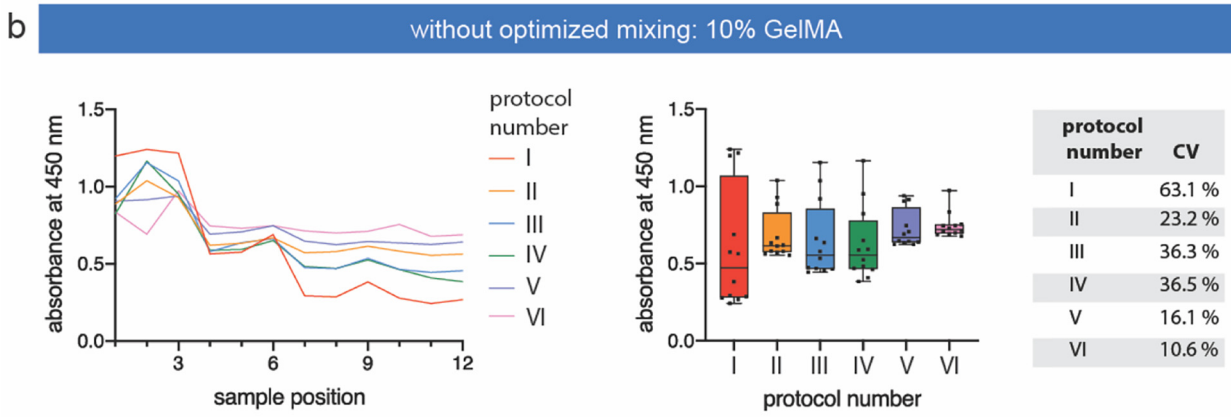

protocol number	CV
I	63.1 %
II	23.2 %
III	36.3 %
IV	36.5 %
V	16.1 %
VI	10.6 %

c

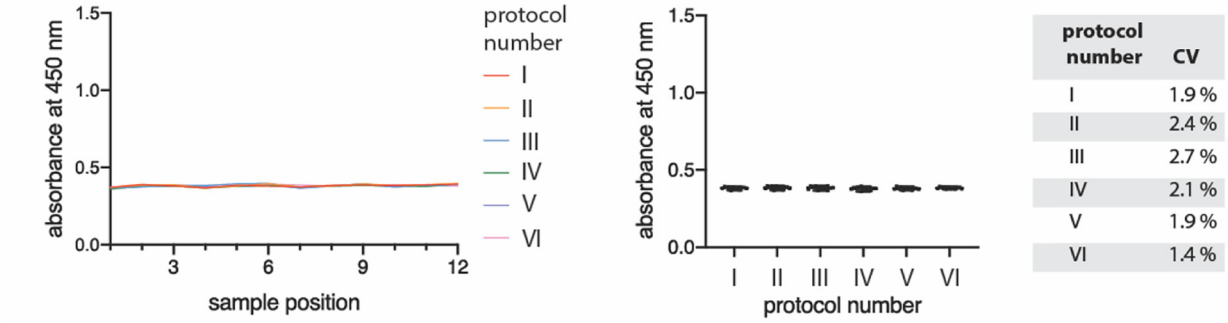

protocol number	CV
I	1.9 %
II	2.4 %
III	2.7 %
IV	2.1 %
V	1.9 %
VI	1.4 %

d

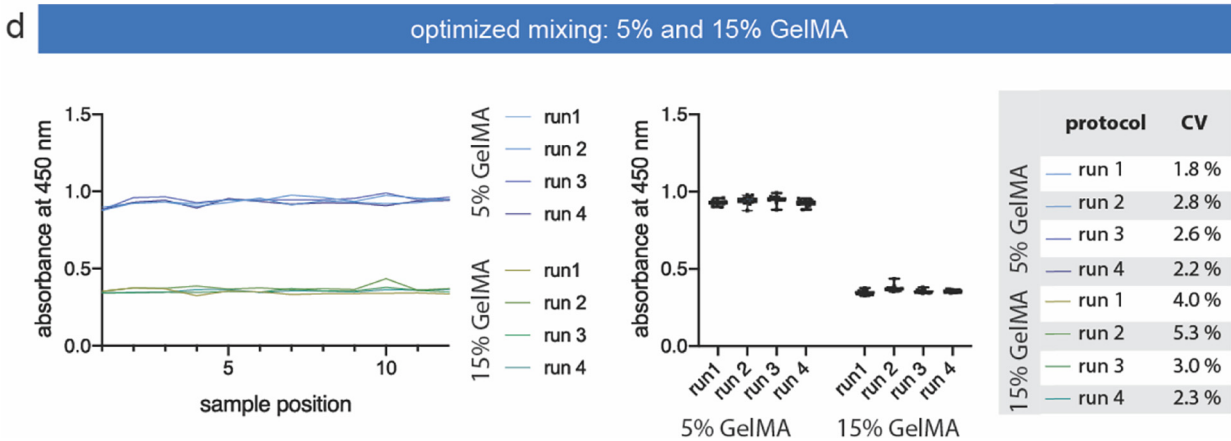

	protocol	CV
5% GelMA	run 1	1.8 %
	run 2	2.8 %
	run 3	2.6 %
	run 4	2.2 %
15% GelMA	run 1	4.0 %
	run 2	5.3 %
	run 3	3.0 %
	run 4	2.3 %

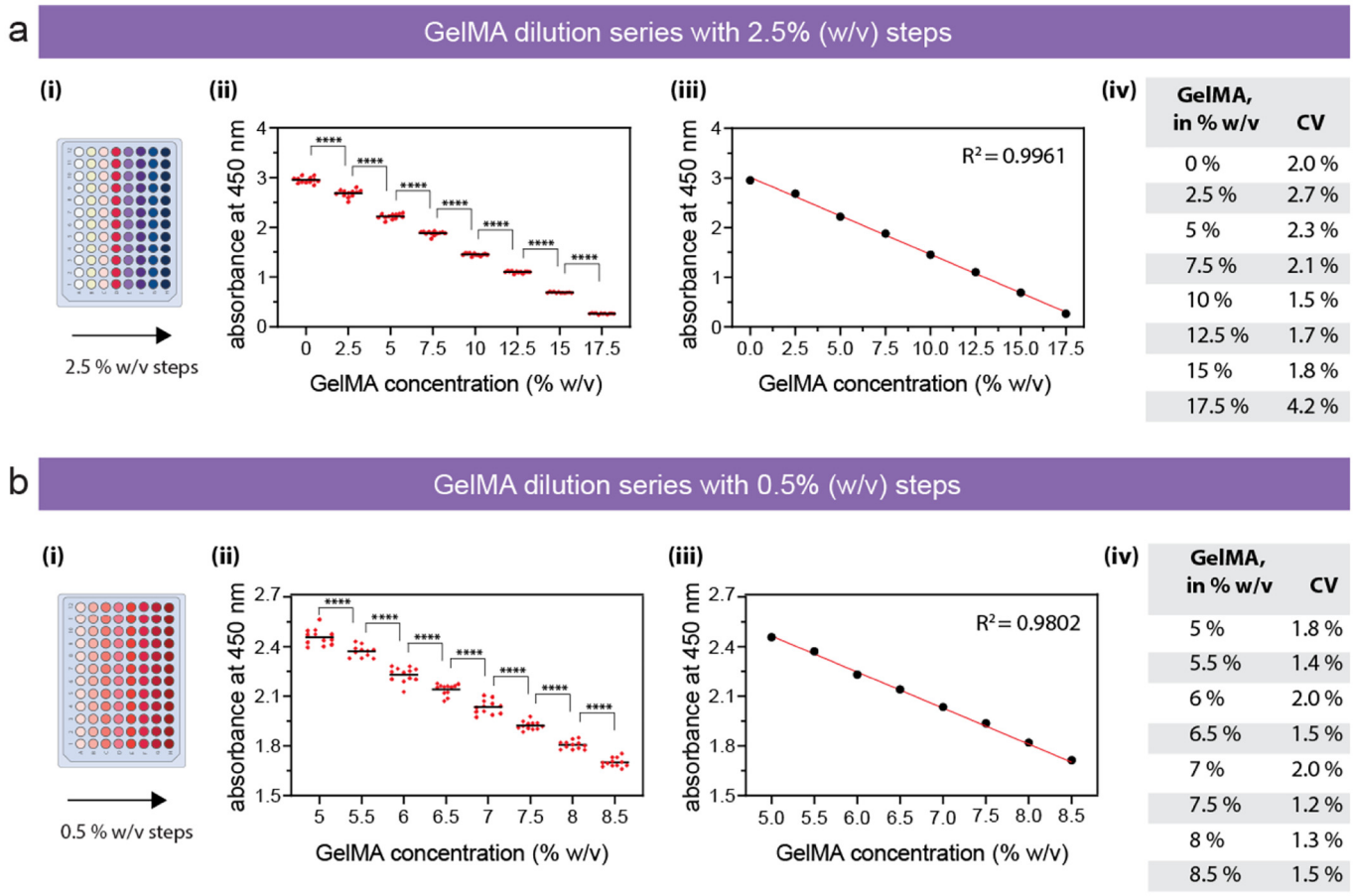

Fig. 5. Application of the workstation to generate GelMA serial dilutions. A GelMA dilution series was generated with (a) 2.5% and (b) 0.5% (*w*/*v*) steps to demonstrate the automated production capabilities for hydrogel-based 3D constructs in 96-well plates and the reproducibility of the workflow ($n = 12$ per GelMA concentration). Absorbance measurements at 450 nm are shown as well as the linear regression model with the calculation of R^2. The CV (coefficient of variation) value is listed for each manufactured concentration step. Means ± standard deviations, ****$P < 0.0001$.

demonstrated an excellent fit with an R^2 value of 0.9961 (Fig. 5a/iii), confirming the high reproducibility of the prepared hydrogel precursor solutions. Calculated CV values ranged for the prepared dilutions from 1.5 to 4.2% (Fig. 5a/iv). In addition to the 2.5% (*w*/*v*) dilution series, a 0.5% (*w*/*v*) dilution series was executed to demonstrate the ability to reproducibly prepare and identify very small GelMA concentration steps. To do so, a 20% (*w*/*v*) GelMA stock solution was diluted to GelMA concentrations ranging from 5 to 8.5% (*w*/*v*) in a 96 well plate ($n = 12$ per concentration) (Fig. 5b/i). Absorbance measurements yielded a high significance ($p < 0.0001$) for the 0.5% (*w*/*v*) GelMA concentration steps (Fig. 5b/ii) with a highly reliable fit for the linear regression ($R^2 = 0.9802$) (Fig. 5b/iii). Calculated CV values ranged from 1.2 to 2.0% for each concentration (Fig. 5b/iv). These results confirm the ability to prepare serial dilutions and distinct concentrations with high reproducibility in a fully automated manner. Moreover, the significant difference ($p < 0.0001$) between the 0.5% (*w*/*v*) GelMA steps highlighted the capability to prepare and identify very small GelMA concentration differences.

3.6. Manual and automated generation of double network hydrogels

The conducted experiments confirmed that the optimized mixing tasks enabled a fully automated and highly reproducible generation of GelMA dilutions. To demonstrate the applicability for additional hydrogel systems and the increased reproducibility compared to manual processing, double network hydrogels (Fig. 6a) were generated and pipetted into a 96-well plate in a manual (Fig. 6b) and automated (Fig. 6c) manner ($n = 96$ samples per mode). While there was no significant difference in the mean absorbance values for the manual (0.910 ± 0.137) and automated (0.900 ± 0.036) mode, the calculated CV values decreased from 15.0 (manual) to 4.0% (automated), illustrating a notable decrease in the variations between the two groups (Fig. 6d). Since the *p*-value of an unpaired *t*-test tests the differences between the means of two populations, an f-test was employed to test the equality of the two population variances [55]. The conducted f-test showed significant differences ($p < 0.0001$) between the variances of the manual and automated workflow. These results highlight that the modular

Fig. 4. Summary of experiments to optimize mixing of GelMA. (a) A method was established to identify homogeneous mixtures by measuring the absorbance values of samples from different depths throughout the mixture. (b) Without optimized mixing protocols, absorbance measurements yielded decreasing values with increasing depths ($n = 12$) for the generation of a 10% (*w*/*v*) GelMA precursor solution; measured CV values ranged between 10.6 and 63.1%. (c) The optimized mixing protocol generated absorbance values with minimal deviations, which was confirmed with CV values ranging from 1.4 to 2.7%. (d) By applying the optimized mixing protocol to generate 5% and 15% (*w*/*v*) GelMA precursor solutions, the results showed low CV values and reproducible preparation in four repeats, referred to as run 1–4.

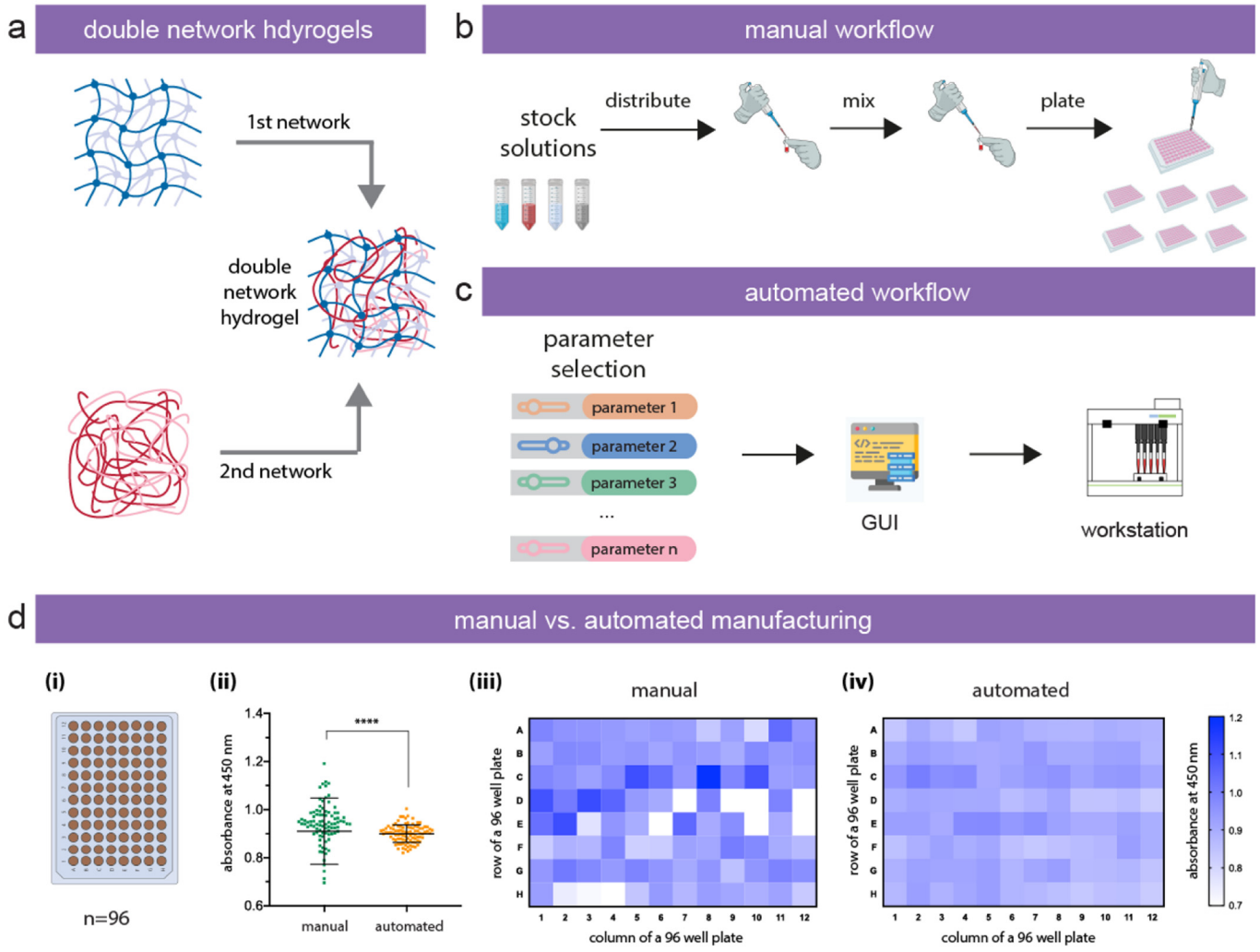

Fig. 6. Application of the workstation to generate double network using 2% (*w*/*v*) alginate and 5% (*w*/*v*) GelMA. (a) A double network hydrogel consists of two polymer networks. For this application, a double network with 5% (*w*/*v*) GelMA and 2% (*w*/*v*) was prepared and crosslinked with 0.15% (*w*/*v*) LAP. (b) While the manual workflow requires various manual-based pipetting and handling steps, (c) the presented workflow is executed in a fully automated manner. (d) A comparison between the manual and automated preparation resulted in decreased CV (coefficient of variation) values from 14.1% (manual) to 4% (automated) ($n = 96$). Means ± standard deviations, $^{****}P < 0.0001$.

workstation enables the preparation and production of hydrogel-based 3D constructs with increased reproducibility compared to manual handling. In contrast to manual workflows, optimized and established protocols can be easily upscaled to produce hundreds of hydrogels for large scale library screenings [56,57].

The platform provides a flexible setup that allows users to prepare an excessive amount of hydrogel solutions for large-scale studies as well as to use minimal volumes for small-scale studies with expensive materials. In the presented studies, stock solutions of around 10 to 15 mL were used to prepare GelMA-based dilution series with volumes of 3 to 5 mL. These dilutions were used to demonstrate the ability to prepare defined and tailored samples into 96-well plates in a reproducible manner. Hence, such a workflow can be used in the future to enable mechanobiology studies to identify the influence of stiffness changes on cellular changes [8]. Given the ability to produce hundreds of samples, such high-throughput studies open up new avenues to screen different parameter combinations with the aim of identifying an optimal parameter set for a given target, such as increased osteogenic differentiation [22]. Next to high-throughput studies, the customizable setup with the exchangeable pipetting set also allows small-scale studies with minimal volume. For example, the smallest pipette size with a volume range of 1–10 μL can be implemented to aspirate small volumes from a stock solution directly into a well plate. Such a capability is especially required for adding growth factors to the cells. Given the flexibility, the storage module can be easily integrated to increase throughput. If not, the setup can be also used only for one plate and simple tasks, such as media exchange (Supplementary Video 3). By applying an open-source approach that is accessible to research labs around the world, the budget does not become an access barrier and the technology can be used for all sorts of studies.

3.7. Establishment of a parameter library to predict mechanical properties of GelMA

A parameter library was generated to predict and subsequently manufacture mechanically defined hydrogel properties with a given parameter set. Since the stiffness of the hydrogel is mainly regulated by the polymer concentration and the crosslinking parameters [1], the parameter library was generated by systematically studying the influence of the GelMA concentration (in *w*/*v*), light exposure duration (in seconds), and light intensity (in mW/cm^2) on the compressive moduli (in kPa). To do this, a methodology was developed to systematically characterize the multidimensional parameter window of a polymer network using the developed automated workflow to generate a parameter library

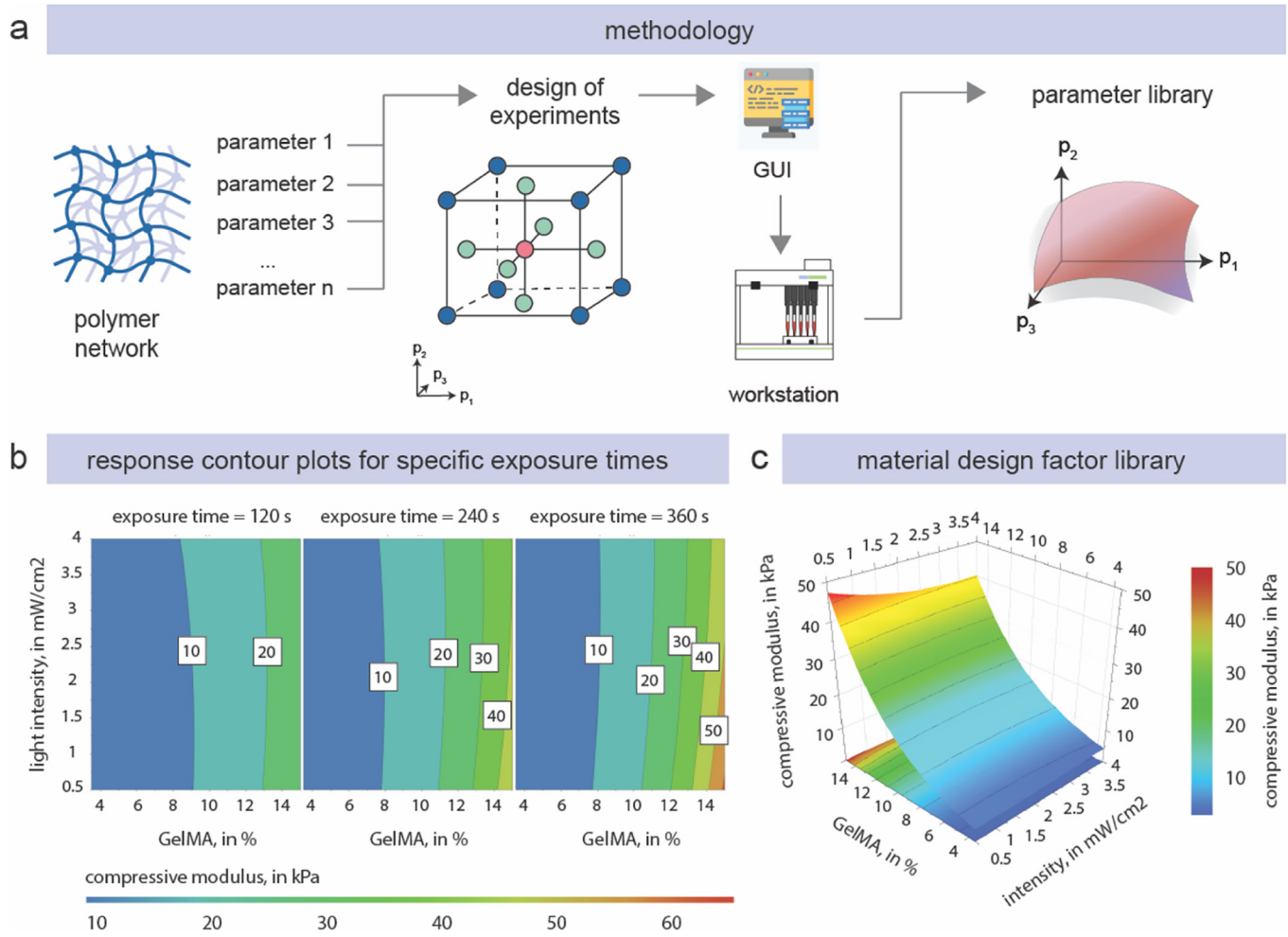

Fig. 7. Application of a Design of Experiments approach to generate a parameter library for GelMA. (a) A methodology is presented to systematically characterize the multidimensional parameter window of a polymer network using the developed automated workflow to generate a parameter library. A Box-Behnken design is applied for response surface methodology with the following material design factors: light intensity (mW/cm^2), GelMA concentration (% (*w*/*v*)), and exposure time (s). (b) Differences in the compressive moduli in respect to the light intensities are displayed as response contour plots for the following exposure times: 120, 240, 360 s. (c) A GelMA material design factor library was generated and the response surface of the compressive moduli (kPa) is illustrated with varying GelMA concentrations and light intensities.

(Fig. 7/a). The experimental setup was organized following a Design of Experiment (DoE) approach to select a representative set of experiments and to identify the influence of each parameter. The results are shown as 2D response surface plots mapped for three light intensities (Fig. 7/b) and as a 3D response surface plot of the compressive modulus (Fig. 7/c). The plots indicate that the concentration of GelMA has the highest influence on the compressive moduli, and exposure time and light intensity only exhibit a minor influence. Statistical analysis of the acquired model yielded an accurate fit with an R^2 value of 0.917. The software application, used to analyze and model the data, calculated a model validity of 0.827, indicating that there were no statistically relevant model problems, such as the presence of outliers, an incorrect model, or a transformation problem. The reproducibility indicator compared the variation of the replicates compared to the overall variability and indicated a high reproducibility with 0.907. With the generated model, the compressive modulus for a given parameter setup can be predicted to accelerate the production of mechanically defined hydrogel properties without tedious preliminary experiments. The option to biofabricate in high-throughput mode and obtain reproducible mechanically defined hydrogels is in high demand in the biomedical community in the form of studies addressing matrix stiffness and cellular functions [8]. Additional information on the observed vs predicted results as well as on the factor effects are provided in the Supplementary Fig. 6 and 7.

3.8. Limitations

The study focused on the engineering of a platform technology to provide fully automated workflows from hydrogel precursors solutions to crosslinked hydrogels as well as the validation with GelMA-based hydrogels in four experiments. The experiments were conducted to, firstly, study the material design factors of GelMA-based hydrogels with a DoE-approach and, secondly, demonstrate the ability to conduct high-throughput studies with increased reproducibility compared to manual handling. It is beyond the scope of this work to integrate additional hydrogels. Hence, in future studies, the presented platform should be applied to other natural, synthetic and semi-synthetic hydrogel systems as well as other crosslinking methods. This would be in particular interesting to demonstrate the broad application range as well as to study the time savings compared to manual tasks. Next, the pipetting performance has to be validated not only with water and glycerol, but also with hydrogels used in the hydrogel-specific applications. While the current study evaluates water and glycerol, the pipetting precision and accuracy need to be studied also for GelMA and related hydrogel systems. Finally, the equations of the DoE study have not been verified by predicting a formulation to design a pre-determined compressive modulus, producing the samples and validating how close the result comes to the predicted output.

4. Conclusion

In summary, we report an open-source technology platform to increase the throughput and reproducibility of hydrogel biofabrication workflows and to establish a methodology to investigate the combinatorial effects of the material and process parameters. Supported by an in-house developed protocol design app, users are guided through the parameter selection process to generate a ready-to-use protocol script to operate the presented workstation. The conceptualized workstation builds upon an assembly line approach and includes specific modules and functionalities required for hydrogel processing tasks. By combining pipetting capabilities for non-viscous and viscous materials, the platform enables researchers to prepare defined hydrogel precursor solutions and manufacture photo-crosslinked 3D constructs in a reproducible and efficient manner. The platform was successfully applied to prepare defined GelMA serial dilutions and double network hydrogel constructs with a high reproducibility without human intervention. The integration of DoE approaches facilitated a systematic study of the material and process parameters to establish a parameter library. This methodology enables an accelerated and reproducible approach to screen hydrogel parameter combinations for a detailed understanding of the hydrogel systems, resulting in greater predictive power of defined material design factors. Building upon the presented open-source approach, researchers have the ability to modify hardware features, customize software code, and share the new developments with the wider community.

Declaration of Competing Interest

CM and DWH are founders and shareholders of Gelomics Pty Ltd. CM is also Managing Director of Gelomics Pty Ltd. The authors have no other relevant affiliations or financial involvement with any organization or entity with a financial interest in or financial conflict with the subject matter or materials discussed in the manuscript apart from those disclosed.

Acknowledgment

The authors acknowledge the members of the Centre in Regenerative Medicine at QUT, in particular, Antonia Horst and Pawel Mieszczanek for their helpful suggestions and feedback. This work was supported by the QUT's Postgraduate Research Award for SE and MK, and by the Australian Research Council (ARC) under grant agreement IC160100026 (ARC Industrial Transformation Training Centre in Additive Biomanufacturing). We thank Prakash Adhikari and Andrew J. Zele (QUT Centre for Vision and Eye Research) for the spectroradiometric measurements. OF and MK received mobility support through the German Academic Exchange Service (DAAD ##57445433). The authors appreciate valuable and constructive suggestions from the anonymous reviewers and editor. BioRender supported the figure generation.

Appendix A. Supplementary data

Supplementary data to this article can be found online at https://doi.org/10.1016/j.matdes.2021.109619.

References

[1] J. Malda, et al., 25th anniversary article: engineering hydrogels for biofabrication, Adv. Mater. 25 (36) (2013) 5011–5028, https://doi.org/10.1002/adma.201302042.
[2] N. Annabi, et al., 25th anniversary article: rational design and applications of hydrogels in regenerative medicine, Adv. Mater. 26 (1) (2014) 85–124, https://doi.org/10.1002/adma.201303233.
[3] P. Calvert, Hydrogels for soft machines, Adv. Mater. 21 (7) (2009) 743–756, https://doi.org/10.1002/adma.200800534.
[4] M. Lee, R. Rizzo, F. Surman, M. Zenobi-Wong, Guiding lights: Tissue bioprinting using photoactivated materials, Chem. Rev. (2020) https://doi.org/10.1021/acs.chemrev.0c00077 acs.chemrev.0c00077.
[5] N. Gjorevski, et al., Designer matrices for intestinal stem cell and organoid culture, Nature. 539 (7630) (2016) 560–564, https://doi.org/10.1038/nature20168.
[6] M.J. Kratochvil, A.J. Seymour, T.L. Li, S.P. Paşca, C.J. Kuo, S.C. Heilshorn, Engineered materials for organoid systems, Nat. Rev. Mater. 4 (9) (2019) 606–622, https://doi.org/10.1038/s41578-019-0129-9.
[7] K.S. Lim, J.H. Galarraga, X. Cui, G.C.J. Lindberg, J.A. Burdick, T.B.F. Woodfield, Fundamentals and applications of photo-cross-linking in bioprinting, Chem. Rev. (2020) https://doi.org/10.1021/acs.chemrev.9b00812 acs.chemrev.9b00812.
[8] C. Kim, et al., Stem cell mechanosensation on gelatin methacryloyl (GelMA) stiffness gradient hydrogels, Ann. Biomed. Eng. 48 (2) (2020) 893–902, https://doi.org/10.1007/s10439-019-02428-5.
[9] N.A. Peppas, J.Z. Hilt, A. Khademhosseini, R. Langer, Hydrogels in biology and medicine: from molecular principles to bionanotechnology, Adv. Mater. 18 (11) (2006) 1345–1360, https://doi.org/10.1002/adma.200501612.
[10] T.J. Hinton, et al., Three-dimensional printing of complex biological structures by freeform reversible embedding of suspended hydrogels, Sci. Adv. 1 (9) (2015), e1500758, https://doi.org/10.1126/sciadv.1500758.
[11] D.B. Kolesky, R.L. Truby, A.S. Gladman, T.A. Busbee, K.A. Homan, J.A. Lewis, 3D bioprinting of vascularized, heterogeneous cell-laden tissue constructs, Adv. Mater. 26 (19) (2014) 3124–3130, https://doi.org/10.1002/adma.201305506.
[12] A.S. Gladman, et al., Biomimetic 4D printing, Nat. Mater. 15 (4) (2016) 413–418, https://doi.org/10.1038/nmat4544.
[13] S. Eggert, D.W. Hutmacher, In vitro disease models 4.0 via automation and high-throughput processing, Biofabrication 11 (4) (2019) 043002, https://doi.org/10.1088/1758-5090/ab296f.
[14] K. Olsen, The first 110 years of laboratory automation, J. Lab. Autom. 17 (6) (2012) 469–480, https://doi.org/10.1177/2211068212455631.
[15] R.D. King, et al., The automation of science, Science. 324 (5923) (2009) 85–89, https://doi.org/10.1126/science.1165620.
[16] D.P. Tabor, et al., Accelerating the discovery of materials for clean energy in the era of smart automation, Nat. Rev. Mater. 3 (5) (2018) 5–20, https://doi.org/10.1038/s41578-018-0005-z.
[17] K. Sanderson, Automation: chemistry shoots for the moon, Nature. 568 (7753) (2019) 577–579, https://doi.org/10.1038/d41586-019-01246-y.
[18] N. Blow, Lab automation: tales along the road to automation, Nat. Methods 5 (1) (2008) 109–112, https://doi.org/10.1038/nmeth0108-109.
[19] I.T. Ozbolat, K.K. Moncal, H. Gudapati, Evaluation of bioprinter technologies, Addit. Manuf. 13 (2017) 179–200, https://doi.org/10.1016/j.addma.2016.10.003.
[20] I.T. Ozbolat, M. Hospodiuk, Current advances and future perspectives in extrusion-based bioprinting, Biomaterials. 76 (2016) 321–343, https://doi.org/10.1016/j.biomaterials.2015.10.076.
[21] P.D. Dalton, T.B.F. Woodfield, V. Mironov, J. Groll, Advances in hybrid fabrication toward hierarchical tissue constructs, Adv. Sci. 1902953 (2020) 1902953, https://doi.org/10.1002/advs.201902953.
[22] A.D. Pirouz, et al., A combinatorial cell-laden gel microarray for inducing osteogenic differentiation of human mesenchymal stem cells, Sci. Rep. 4 (2015) 1–9, https://doi.org/10.1038/srep03896.
[23] S. Gobaa, S. Hoehnel, M. Roccio, A. Negro, S. Kobel, M.P. Lutolf, Artificial niche microarrays for probing single stem cell fate in high throughput, Nat. Methods 8 (11) (2011) 949–955, https://doi.org/10.1038/nmeth.1732.
[24] D.G. Anderson, S. Levenberg, R. Langer, Nanoliter-scale synthesis of arrayed biomaterials and application to human embryonic stem cells, Nat. Biotechnol. 22 (7) (2004) 863–866, https://doi.org/10.1038/nbt981.
[25] D.G. Anderson, D. Putnam, E.B. Lavik, T.A. Mahmood, R. Langer, Biomaterial microarrays: rapid, microscale screening of polymer-cell interaction, Biomaterials. 26 (23) (2005) 4892–4897, https://doi.org/10.1016/j.biomaterials.2004.11.052.
[26] M. Rimann, B. Angres, I. Patocchi-Tenzer, S. Braum, U. Graf-Hausner, Automation of 3D cell culture using chemically defined hydrogels, J. Lab. Autom. 19 (2) (2014) 191–197, https://doi.org/10.1177/2211068213508651.
[27] E.A. Brooks, L.E. Jansen, M.F. Gencoglu, A.M. Yurkevicz, S.R. Peyton, Complementary, semiautomated methods for creating multidimensional PEG-based biomaterials, ACS Biomater. Sci. Eng. 4 (2) (2018) 707–718, https://doi.org/10.1021/acsbiomaterials.7b00737.
[28] S. Eggert, M. Kahl, R. Kent, N. Bock, C. Meinert, D.W. Hutmacher, An open source technology platform to manufacture hydrogel-based 3D culture models in an automated and standardized fashion, J. Vis. Exp. (2020) https://doi.org/10.3791/61261 e61261.
[29] W. Schuurman, et al., Gelatin-methacrylamide hydrogels as potential biomaterials for fabrication of tissue-engineered cartilage constructs, Macromol. Biosci. 13 (5) (2013) 551–561, https://doi.org/10.1002/mabi.201200471.
[30] S.A. Weissman, N.G. Anderson, Design of Experiments (DoE) and process optimization. A review of recent publications, Org. Process. Res. Dev. 19 (11) (2015) 1605–1633, https://doi.org/10.1021/op500169m.
[31] J. Usprech, D.A. Romero, C.H. Amon, C.A. Simmons, Combinatorial screening of 3D biomaterial properties that promote myofibrogenesis for mesenchymal stromal cell-based heart valve tissue engineering, Acta Biomater. 58 (2017) 34–43, https://doi.org/10.1016/j.actbio.2017.05.044.
[32] W.L.K. Chen, M. Likhitpanichkul, A. Ho, C.A. Simmons, Integration of statistical modeling and high-content microscopy to systematically investigate cell-substrate interactions, Biomaterials. 31 (9) (2010) 2489–2497, https://doi.org/10.1016/j.biomaterials.2009.12.002.
[33] S. Eggert, P. Mieszczanek, C. Meinert, D.W. Hutmacher, OpenWorkstation: a modular open-source technology for automated in vitro workflows, HardwareX. 8 (2020), e00152, https://doi.org/10.1016/j.ohx.2020.e00152.

[34] International Organization for Standardization Piston-operated volumetric apparatus: Part 2: Piston Pipettes, ISO 8655-2:2002. Vernier, Geneva, Switzerland, http://www.sartorius.co.rs/contentFiles/files/ISO_8655-2_2002.pdf 2002.
[35] A. Volk, C.J. Kähler, Density model for aqueous glycerol solutions, Exp. Fluids 59 (5) (2018) 75, https://doi.org/10.1007/s00348-018-2527-y.
[36] D. Loessner, et al., Functionalization, preparation and use of cell-laden gelatin methacryloyl–based hydrogels as modular tissue culture platforms, Nat. Protoc. 11 (4) (2016) 727–746, https://doi.org/10.1038/nprot.2016.037.
[37] D. Schneidereit, L. Kraus, J.C. Meier, O. Friedrich, D.F. Gilbert, Step-by-step guide to building an inexpensive 3D printed motorized positioning stage for automated high-content screening microscopy, Biosens. Bioelectron. 92 (August 2016) (2017) 472–481, https://doi.org/10.1016/j.bios.2016.10.078.
[38] P. Almada, et al., Automating multimodal microscopy with NanoJ-fluidics, Nat. Commun. 10 (1) (2019) 1223, https://doi.org/10.1038/s41467-019-09231-9.
[39] B.T. Wittbrodt, D.A. Squires, J. Walbeck, E. Campbell, W.H. Campbell, J.M. Pearce, Open-source photometric system for enzymatic nitrate quantification, PLoS One 10 (8) (2015), e0134989, https://doi.org/10.1371/journal.pone.0134989.
[40] G. Glotz, C.O. Kappe, Design and construction of an open source-based photometer and its applications in flow chemistry, React. Chem. Eng. 3 (4) (2018) 478–486, https://doi.org/10.1039/C8RE00070K.
[41] T. Akam, M.E. Walton, pyPhotometry: Open source Python based hardware and software for fiber photometry data acquisition, Sci. Rep. 9 (1) (2019) 3521, https://doi.org/10.1038/s41598-019-39724-y.
[42] S. Oliver, L. Zhao, A.J. Gormley, R. Chapman, C. Boyer, Living in the fast lane—high throughput controlled/living radical polymerization, Macromolecules. 52 (1) (2019) 3–23, https://doi.org/10.1021/acs.macromol.8b01864.
[43] R.A. Plenderleith, et al., Arginine–glycine–aspartic acid functional branched semi-interpenetrating hydrogels, Soft Matter 11 (38) (2015) 7567–7578, https://doi.org/10.1039/C5SM00695C.
[44] J.R. Johnson, et al., GeneMill: a 21st century platform for innovation, Biochem. Soc. Trans. 44 (3) (2016) 681–683, https://doi.org/10.1042/BST20160012.
[45] M. May, A DIY approach to automating your lab, Nature. 569 (7757) (2019) 587–588, https://doi.org/10.1038/d41586-019-01590-z.
[46] S.L. Vega, et al., Combinatorial hydrogels with biochemical gradients for screening 3D cellular microenvironments, Nat. Commun. 9 (1) (2018) 614, https://doi.org/10.1038/s41467-018-03021-5.
[47] S. Pahoff, C. Meinert, O. Bas, L. Nguyen, T.J. Klein, D.W. Hutmacher, Effect of gelatin source and photoinitiator type on chondrocyte redifferentiation in gelatin methacryloyl-based tissue-engineered cartilage constructs, J. Mater. Chem. B 7 (10) (2019) 1761–1772, https://doi.org/10.1039/C8TB02607F.
[48] L. Bessemans, et al., Automated gravimetric calibration to optimize the accuracy and precision of TECAN freedom EVO liquid handler, J. Lab. Autom. 21 (5) (2016) 693–705, https://doi.org/10.1177/2211068216632349.
[49] G. Lippi, G. Lima-Oliveira, G. Brocco, A. Bassi, G.L. Salvagno, Estimating the intra- and inter-individual imprecision of manual pipetting, Clin. Chem. Lab. Med. 55 (7) (2017) 962–966, https://doi.org/10.1515/cclm-2016-0810.
[50] D.N. Joyce, J.P.P. Tyler, Accuracy, precision and temperature dependence of disposable tip pipettes, Med. Lab. Technol. 30 (4) (1973) 331–334https://www.ncbi.nlm.nih.gov/pubmed/4803941.
[51] C.D. O'Connell, et al., Tailoring the mechanical properties of gelatin methacryloyl hydrogels through manipulation of the photocrosslinking conditions, Soft Matter 14 (11) (2018) 2142–2151, https://doi.org/10.1039/C7SM02187A.
[52] A.D. Arya, et al., Gelatin methacrylate hydrogels as biomimetic three-dimensional matrixes for modeling breast cancer invasion and chemoresponse in vitro, ACS Appl. Mater. Interfaces 8 (34) (2016) 22005–22017, https://doi.org/10.1021/acsami.6b06309.
[53] I. Pepelanova, K. Kruppa, T. Scheper, A. Lavrentieva, Gelatin-methacryloyl (GelMA) hydrogels with defined degree of functionalization as a versatile toolkit for 3D cell culture and extrusion bioprinting, Bioengineering. 5 (3) (2018) 55, https://doi.org/10.3390/bioengineering5030055.
[54] B.J. Klotz, D. Gawlitta, A.J.W.P. Rosenberg, J. Malda, F.P.W. Melchels, Gelatin-methacryloyl hydrogels: towards biofabrication-based tissue repair, Trends Biotechnol. 34 (5) (2016) 394–407, https://doi.org/10.1016/j.tibtech.2016.01.002.
[55] G.W. Snedecor, W.G. Cochran, Statistical Methods, Iowa State University Press, 1989.
[56] D.G. Anderson, D.M. Lynn, R. Langer, Semi-automated synthesis and screening of a large library of degradable cationic polymers for gene delivery, Angew. Chem. Int. Ed. 42 (27) (2003) 3153–3158, https://doi.org/10.1002/anie.200351244.
[57] C.A. Tweedie, D.G. Anderson, R. Langer, K.J. Van Vliet, Combinatorial material mechanics: high-throughput polymer synthesis and nanomechanical screening, Adv. Mater. 17 (21) (2005) 2599–2604, https://doi.org/10.1002/adma.200501142.